In Cellulo Light-Induced Dynamics in a BODIPY-Perylene Dyad

Tingxiang Yang,[a, b] Ruben Arturo Arellano-Reyes,[c] Rhianne C. Curley,[c] Keshav Kumar Jha,[a, b] Avinash Chettri,[a, b] Tia E. Keyes,[c] and Benjamin Dietzek-Ivanšić*[a, b]

Abstract: BODIPY-based donor-acceptor dyads are widely used as sensors and probes in life science. Thus, their biophysical properties are well established in solution, while their photophysical properties *in cellulo*, i.e., in the environment, in which the dyes are designed to function, are generally understood less. To address this issue, we present a sub-ns time-resolved transient absorption study of the excited-state dynamics of a BODIPY-perylene dyad designed as a twisted intramolecular charge transfer (TICT) probe of the local viscosity in live cells.

Introduction

BODIPY (boron-dipyrromethene) based donor-acceptor (D–A) dyads have been developed for bio-imaging and sensing, for example for visualizing and targeting the localization of cellular compartments and biomolecules, such as amino acids and proteins,[1] as well as for photodynamic therapy.[2] It was shown that the photochemical and photophysical properties of these BODIPY dyads vary significantly with the environment.[3] In non-polar solvents, the energy of charge-separated (CS) states in D–A dyads are usually raised with respect to localized singlet excited (LE) states. As a consequence, the excited-state relaxation upon photoexcitation to the LE state does bypass the CS state, which is energetically not accessible.[4] Upon increasing the solvent polarity, the energy of the CS decreases and it partakes in excited state relaxation, i.e., populating the CS becomes thermodynamically feasible upon optical excitation of the LE states. The resultant radical ion-pair can persist for prolonged times, i.e., up to a few ns.[5] The choice of solvent also determines the tendency of BODIPY derivatives to aggregate. The systems are poorly soluble in water and hence aggregate in solvent mixtures with a high water fraction.[6] As aggregation changes the orientation and structural flexibility of the acceptor unit with respect to the BODIPY core, BODIPY D–A dyads are rather emissive in their aggregated state.[7] Similarly, increasing the solvent viscosity can strongly suppress the non-radiative decay of the excited states in such dyads.[8]

While the photophysical properties of BODIPY D–A dyads are known to critically depend on the solvent properties, photophysical studies focusing on complex environmental effects, as, for example, presented by the complex cellular environment, are lacking. Only fluorescence lifetime imaging has been applied to monitor the decay of the emissive state in BODIPY D–A rotors in cells to date.[9] To add to the FLIM studies with a specific focus on the fast, sub-ns light-induced processes, we studied **BODIPY-Per** (Figure 1a) by sub-ps time-resolved transient absorption (TA) spectroscopy *in cellulo*. These probes with red emissions were designed for triplet-triplet annihilation upconversion.

Results and Discussion

As a basis for the *in cellulo* studies, Figure 1 depicts the chemical structure of **BODIPY-Per** together with its absorption and emission spectra in DMSO/ water mixtures. Like many other BODIPY derivates, **BODIPY-Per** is completely insoluble in water and only dissolved when organic solvent is present. **BODIPY-Per** features a maximum absorption at 532 nm in DMSO. The maximum slightly redshifts to 535 nm when a water fraction of up to 50 % is reached. This redshift is accompanied by the weakened intensity and a band broadening (Figures 1a and S1a). Figure 1b indicates that **BODIPY-Per** scarcely emits in DMSO, whereas a red emission evolves as the water fraction (f_w) increases. At low f_w a peak centered around 560 nm is observed (Figure 1b), which originates from the emission of the LE state.[9b,10] This emission band is gradually quenched with the increasing concentrations of **BODIPY-Per** (Figure S1b), implying intermolecular interactions quenching the **BODIPY-Per** LE emission, likely due to aggregate formation.[11] This is in line

[a] T. Yang, K. K. Jha, A. Chettri, Prof. Dr. B. Dietzek-Ivanšić
Leibniz Institute of Photonic Technology (Leibniz-IPHT)
Albert-Einstein-Street 9, 07745 Jena (Germany)
E-mail: benjamin.dietzek@leibniz-ipht.de

[b] T. Yang, K. K. Jha, A. Chettri, Prof. Dr. B. Dietzek-Ivanšić
Institute of Physical Chemistry
Friedrich Schiller University Jena
Helmholtzweg 4, 07743 Jena (Germany)

[c] R. A. Arellano-Reyes, R. C. Curley, Prof. Dr. T. E. Keyes
School of Chemical Sciences and National Centre for Sensor Research
Dublin City University
Glasnevin, Dublin 9 (Ireland)

Chemistry–A European Journal

Research Article
doi.org/10.1002/chem.202300224

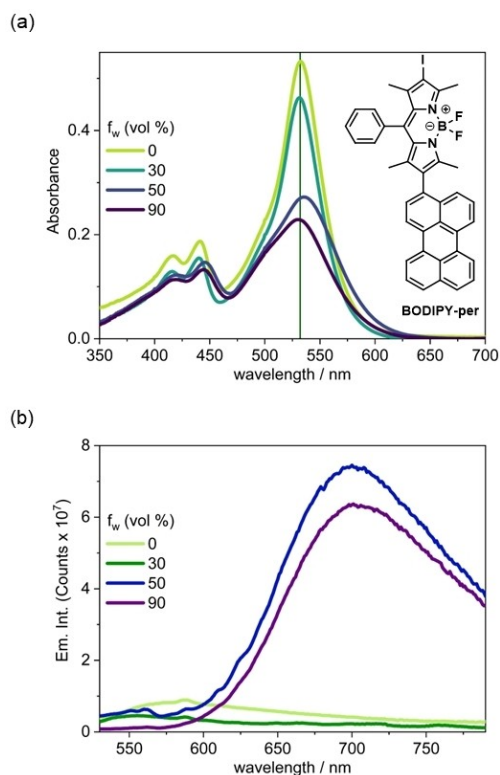**Chemistry Europe**
European Chemical
Societies Publishing

Figure 1. UV/ vis (a) and emission spectra ($\lambda_{ex} = 500$ nm) (b) of **BODIPY-Per** (10 µM) in DMSO/water mixtures with different fractions of water (f_w). Insert in (a) is the molecular structure of **BODIPY-Per** used in this study.

with the simultaneously developing broad emission band at 700 nm, which is typical for aggregation-induced emission.[12] The observed variation of the absorption and emission spectra of **BODIPY-Per** upon varying f_w indicates environmentally-induced changes of the excited-state topology, which might manifest itself also in modified transient absorption data when recorded *in cellulo* (see below).

The uptake of **BODIPY-Per** into human MCF-7 cells was monitored by confocal fluorescence microscopy. MCF-7 cells were incubated in RPMI-1640 cell culture medium containing 10-µM **BODIPY-Per** at a temperature of 37 °C under an atmosphere containing 5% CO_2 for ca. 17 h. To contrast the localization of **BODIPY-Per**, Hoechst 33342 was added to the cells in phenol red free RPMI medium after carefully washing the cells twice with PBS. The emission distributions (Figures 2 and S2) indicate that **BODIPY-Per** accumulates preferentially in the cytoplasm, i.e., out of the nucleus. Similar observations were made for other BODIPY derivatives.[13] To estimate the cytotoxicity of **BODIPY-Per** the alamarBlue (resazurin) assay was employed by adding 10% resazurin in culture medium to the cells in a 96-well plate and incubating for 5 h.[14] Following the 17-h staining with **BODIPY-Per**, the viability of the MCF-7 cells was evaluated under dark and light conditions (Figure 3). Cell viability was assessed by incubating the cells for a further 24 h and 5 h with alamarBlue after the removal of **BODIPY-Per** to allow for cell recovery (see Scheme S1). When kept in the dark, comparably high viabilities of >90% indicate low toxicity in the concentration range of up to 50 µM. However, the cell viability
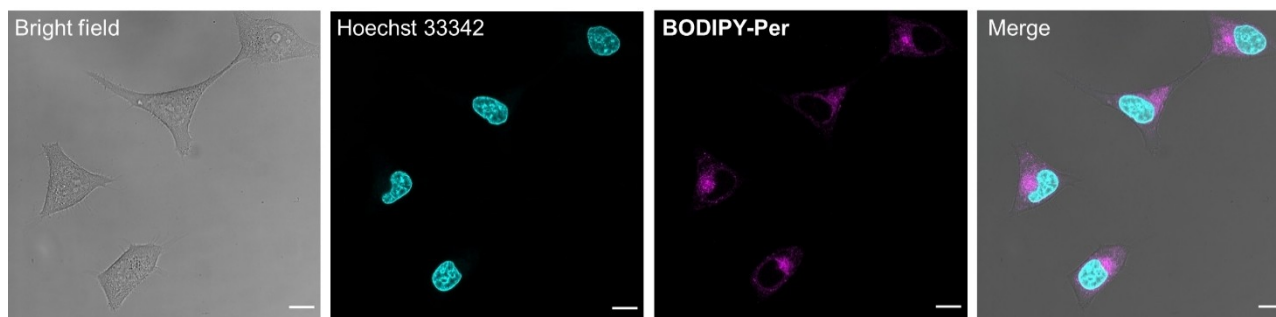

Figure 2. Confocal fluorescence microscopy images of MCF-7 cells co-stained with Hoechst 33342 (1.78 µM, 20 min) and **BODIPY-Per** (10 µM, 17 h). Scale bar: 20 µm.
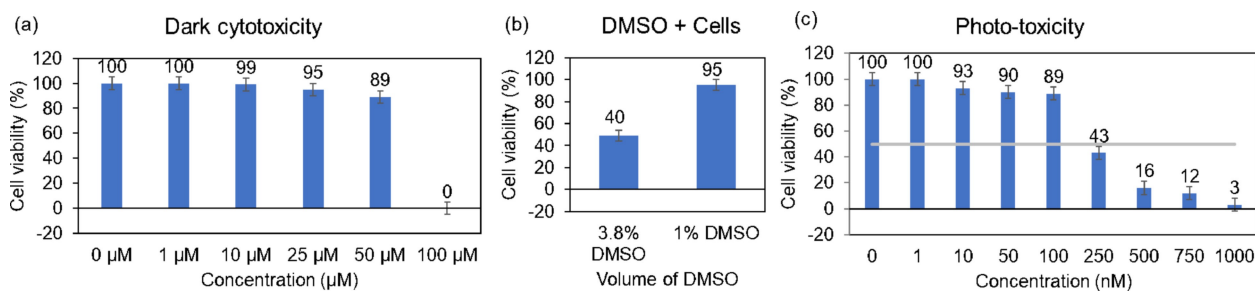

Figure 3. Cell viability of MCF-7 cells determined by alamarBlue assay 24 h after the first 17 h incubating with **BODIPY-Per** at different concentrations without (a) or with (c) extra light irradiation (470 nm LED lamp 2.5 ± 0.09 mW/cm², 2 h). (b) is the dark control cytotoxicity with different concentrations of DMSO (without **BODIPY-Per**). The IC50 value (50% of cell viability), the grey straight line in (c), is 235 ± 21.1 nM.

Chemistry–A European Journal

Research Article
doi.org/10.1002/chem.202300224

Chemistry Europe
European Chemical
Societies Publishing

drops to 0% at 100 μM (Figures 3a and S3a). The DMSO content, ca. 3.8%, used to solubilize **BODIPY-Per** might contribute to the reduced viability, i.e., increasing the DMSO content significantly decreases cell viability (Figures 3b and S3b), as reported before for related systems.[15]

Different from the above-described standard protocol to determine (light-induced) cytotoxicity, the *in cellulo* TA experiments (see below) were conducted immediately after staining and washing the cells, i.e., without an additional 22-h incubation period. Therefore, an additional experiment to assess the cell viability immediately after staining: An EVE™ Automated Cell Counter (NanoEnTek) was employed to assess the viability of MCF-7 cells that were seeded in a 6-well plate and treated with 100 μM **BODIPY-Per** for 17 h, then detached by trypsinisation and stained with Trypan Blue, an indicator for intact cell membranes (see Scheme S1). Under dark conditions, the 100 μM **BODIPY-Per** in MCF-7 cells shows high viability (ca. 82%, Figure S4). Similar values are observed for the MCF-7 samples prepared for *in cellulo* TA measurements (see below; here, a cell-viability of 80% immediately after staining was obtained). These results confirm that the MCF-7 cells have good viability immediately after staining with 100 μM **BODIPY-Per**, under the conditions the *in cellulo* TA experiments were conducted even though such conditions eventually lead to cell death over extended incubation time of 29 h (see the above as discussed for the alamarBlue assay). This might be due to the delayed DNA-damage response, which may ultimately lead to cell death, commonly by apoptosis.[16] Nonetheless, understanding the cellular mechanism leading to (photo)cytotoxicity is not the focus of this paper, which rather focuses on the *in cellulo* light-induced dynamics in **BODIPY-Per**. To this end, we chose 100 μM **BODIPY-Per** to treat the cells for 17 h in the TA measurements (see below) to yield sufficient optical density in the cells for a reasonable signal-to-noise ratio of the TA data. As mentioned before, the *in cellulo* TA data were recorded immediately after 17 h of incubation with the dye, a time point at which the cells are fully stained and viable. To ensure the TA

signals were derived from dye inside the cells, the media containing compounds are washed out by PBS and resuspended in Hanks' balanced salt solution (HBSS) before the cellular TA experiments.

Additionally, we compare the overall photon exposure of the stained cells in the *in cellulo* TA experiment and the alamarBlue assay. In the latter, the cells are irradiated by a blue LED (TeleOpto LEDA-X LED driver and array, 2.5 mW/cm², 2 h) to evaluate their phototoxicity. Hence the number of photons to which the cells are exposed can be estimated to 4.3×10^{19} photons/cm². In the *in cellulo* transient absorption experiments, the average photon flux is 3.4×10^{16} cm^{-2}s^{-1}, however, as the overall TA experiment is designed to take only 2 min, the integrated photon exposure amounts to 4.0×10^{18} photons/cm².

To identify suitable probe-wavelengths for the *in cellulo* study, TA spectroscopy of **BODIPY-Per** was performed in DMSO/water mixture and dioxane as solvents. The experimental transient absorption data (Figure 4) were analyzed by global fitting (Figure S8). In DMSO, photoexcitation with 100-fs pump pulses at 530 nm induces a positive differential absorption band at around 350 nm (Figure 4a), which we assign to the absorption of the S_1 state of the BODIPY chromophore (< 1 ps).[17] The adjacent, strong negative transient absorption band at ca. 475–565 nm represents the ground state bleach of the BODIPY absorption.[18] The weak negative differential absorption features below 450 nm are due to ground state bleaching of the perylene unit (see Figure 4a). The coincidence of these features indicates very rapid electron transfer, i.e., within the time resolution of the experiment, from the per-unit to the photoexcited BODIPY. The resultant charge transfer state is directly reflected in the broad positive absorption band peaking at about 600 nm (Figure 4a), which is indicative of the BODIPY radical-anion (BODIPY$^{•-}$)[19] and perylene radical-cation (Pery$^{•+}$).[20] The negative band between 625 and 725 nm (Figure 4b) recorded in the TA data of dioxane indicates stimulated emission from a charge transfer state.[21] This
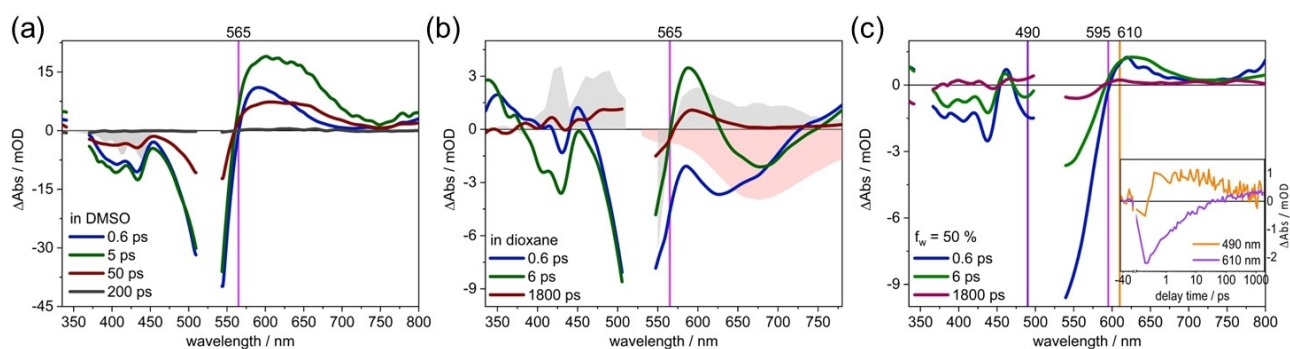

Figure 4. fs transient absorption spectra of **BODIPY-Per** in (a) aerated DMSO (fitted with 3 components: $\tau_1 = 0.5$ *ps*; $\tau_2 = 4$ *ps*; $\tau_3 = 43$ *ps*), (b) deaerated dioxane (fitted with 3 components and a long-lived species: $\tau_1 = 0.3$ *ps*; $\tau_2 = 3$ *ps*; $\tau_3 = 384$ *ps*; τ_4 : long-lived), and (c) in aerated DMSO/water mixture ($f_w = 50\%$) ((fitted with 3 components and a long-lived species: $\tau_1 = 0.2$ *ps*; $\tau_2 = 2$ *ps*; $\tau_3 = 69$ *ps*; τ_4 : long-lived), respectively ($\lambda_{ex} = 530$ nm). See the decay-associated spectra in Figure S8. The grey pattern in (a) is the inverted steady-state absorbance of perylene. The grey pattern in (b) is the spectrum of **BODIPY-Per** recorded at 100 μs delay time, thus reflecting the absorption spectrum of the long-lived triplet state. The pink pattern in (b) is the inverted emission spectrum of **BODIPY-Per** recorded in dioxane. The amplitudes of the inverted steady-state absorbance of perylene in (a), inverted emission spectrum and the 100-μs transient absorption spectrum in (b) are arbitrarily scaled to match the scale of the figure. The insert in (c) is the kinetics probed at selected wavelengths. The spectra are smoothed by Loess method to reduce the electronic noise (the original data are shown in the Figure S6).

fluorescence is essentially quenched in DMSO (Figure 4a), in line with the negligible emission quantum yields Φ_f in DMSO.

In DMSO, the CS state fully develops and undergoes vibrational and structural relaxation within the first 4 ps after photoexcitation, before charge recombination (CR) takes place with a characteristic time constant $\tau_3 = 43$ ps (Figures 4a and S8b). When using dioxane as the solvent, the CS state is much longer lived ($\tau_3 = 384$ ps, Figures 4b and S8a), as the decay kinetics of the CS state in **BODIPY-Per** are strongly affected by the solvent polarity. In the less polar solvent dioxane, the energy of the CS state increases and so does the CS-S_0 energy gap.[22] In contrast, the CS state appears energetically stabilized in highly polar media. This results in a reduced energy gap between the CS and the ground state in DMSO, which in turn facilitates ground state recovery.[17,23]

The differential absorption signature, which persists in the transient absorption signal at 1800 ps (as obtained from fs-time resolved spectroscopy) also extends up to 100 µs (as determined from ns-time resolved transient absorption, Figure 4b). This long lifetime of the differential absorption signature suggests that it reflects the properties of a triplet state. This is further evidenced by the oxygen sensitivity of the signal (Figure S9): In aerated dioxane (as compared to deaerated dioxane), the absorbed intensities decay to zero within 1 µs, which is significantly faster than the one recorded in deaerated dioxane. The oxygen sensitivity of the lifetime points to a triplet state associated with either perylene ($T_1^{Perylene}$) or BODIPY unit (T_1^{BODIPY}) being involved in the excited-state decay.[17,24] Similar observations have been reported for similar charge transfer BODIPY derivatives.[17,20] This microsecond long-lived species are not observed in DMSO as the absorbed signal decay to around zero within 200 ps (Figure 4a). This points out that the yield of the triplet state of **BODIPY-Per** is negligible in DMSO. This is due to the fact that the ^{1}CS state is stabilized in the polar medium, while the T^1 state, corresponding to a locally excited state, is not (see Figure 6). As a consequence of the lower energy of the CS state in the polar medium, there is no driving force to populate the T^1 state in DMSO.

Since water is the majority component in a cell and **BODIPY-Per** is insoluble in water, the photophysical properties of **BODIPY-Per** are studied in DMSO/water mixtures. Upon increasing the water fraction and hence the solvent polarity, the decay of the CS state is accelerated, and its lifetime shortens to 29 ps in a DMSO/water mixture with $f_w = 30\%$ (Figures S7 and S8c). Upon further increasing the water fraction ($f_w = 50\%$), aggregation is induced and the lifetime of the CS state is prolonged to about 67 ps (Figures 4c and S8d). Upon aggregate formation, the differential absorption signature of the zero crossing shifts to 595 nm (for $f_{w=50}$ and 90%) compared to 565 nm in DMSO and dioxane (Figures 4 and S6, S7). This reflects the broader ground-state absorption of **BODIPY-Per** in DMSO water mixtures with high f_w (see Figure 1). A long-lived positive differential absorption band is observed at 460–500 nm for samples dissolved in water/DMSO mixtures with $f_w = 50$ and 90% (Figures 4c and S7d). As shown in the insert of Figure 4c, a significant decay at 610 nm is accompanied by the concomitant growth of a new signal at 490 nm. This feature corresponds to

the absorption of the triplet state in agreement with the reported data of similar BODIPY D–A dyads.[17,20] Thus, from the TA spectra of **BODIPY-Per** recorded from solvent mixtures of different water contents, we conclude that aggregate formation tends to increase the triplet yield from the previously populated CS state.

In the following we will turn to the ultrafast excited state relaxation of **BODIPY-Per**, when incorporated into MCF-7 cells. While the localization and lifetime behaviour of BODIPY-based D–A rotors in a cellular environment have been studied by fluorescence microscopy,[9a,25] *in cellulo* ultrafast transient absorption spectroscopy has not been applied to such dyads in a biological environment. We utilized a time-resolved pump probe setup described earlier.[26] The spectroscopic studies reported in the following, utilize pump pulses centred at 530 nm, while the excited-state dynamics is probed at 580, 650, 700 and 800 nm. These probe-wavelengths are chosen to monitor the population of the CS state. Attempts to use supercontinuum probe pulses failed due to increased scattering from the cells as compared to studies on **BODIPY-Per** solutions. During the *in cellulo* transient absorption experiments, the live MCF-7 cells are exposed to pump light with pulse energies of ca. 26 µJ/cm^2, while the power of the probe beam is typically an order of magnitude lower.

At 580 nm a negative signal appears instantaneously in the *in cellulo* pump-probe kinetics upon photoexcitation (Figure 5a). We ascribe this signal primarily to ground-state bleach although also stimulated emission may contribute at this probe wavelength. Nonetheless, the latter contribution is considered negligible as indicated by the spectral broadening of the absorption spectrum in aqueous environments (Figure 1a) and the negative differential absorption signal in solvent mixtures with $f_w = 50$ and 90% (Figures 4c and S7). In an attempt to capture the excited-state absorption kinetics of the CS state, we shifted the probe wavelengths to 650, 700 and 800 nm (Figures 5b, 5c, and 5d), respectively. Also, at these probe wavelengths we observe negative-only differential absorption signals, corresponding to the emission from the CT state. The stimulated emission contributions in **BODIPY-Per** in MCF-7 cells is comparably short-lived (ca. 20 ps). We associate this short lifetime of the CS state with the decreased CS-S_0 energy gap in the cellular environment and hence – according to energy gap law – an accelerated non-radiative decay. We postulate that interactions of **BODIPY-Per** within the crowded environment in the cells lower the energy of CS state with respect to T_1^{BODIPY} to an extent that population of the triplet becomes impossible (Figure 6). Consequently, no long-lived transient absorption signal is observed. This also indicates that the singlet oxygen generation is not significant *in cellulo*, which is in line with the low photocytotoxicity of **BODIPY-Per** in the transient absorption experiments. This underlines the potential for *in cellulo* TA measurement in understanding light-driven intramolecular processes in fluorescent dyes[27] and photodrugs, as the cellular environment modulates the photophysical process expected to occur based on solution measurements.
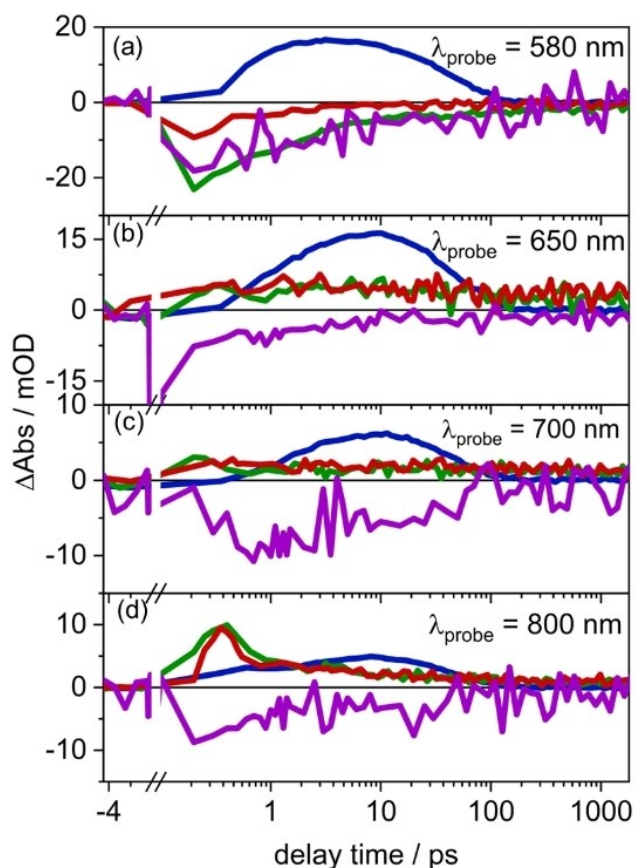
Chemistry–A European Journal

Research Article
doi.org/10.1002/chem.202300224

Chemistry Europe
European Chemical
Societies Publishing

Figure 5. Kinetics of **BODIPY-Per** monitored at 580 nm (a), 650 nm (b), 700 nm (c), 800 nm (d) in different DMSO/water mixtures. In 0% f_w (blue line), in 50% f_w mixture (scale ×500, green line), in 90% f_w mixtures (scale ×500, red line), and in the bulk of live cells (scale ×500, purple line).
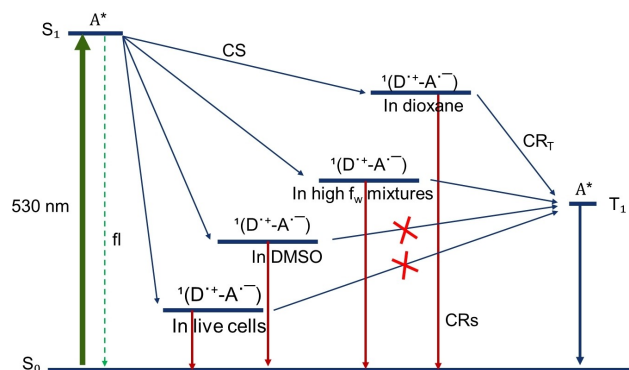

Figure 6. Jablonski diagrams of the photophysical pathway in **BODIPY-Per** in solvents and live cells. Perylene and BODIPY cores act as electron donor (D) and acceptor (A), respectively. fl: fluorescence.

Conclusion

In conclusion, we elucidated the photoinduced dynamics of **BODIPY-Per** in solvents and when taken up by live human cancer cells. The results reveal a remarkable sensitivity of the excited-state dynamics to the local environment of the dyads,

i.e., CS state lifetime relatively shortened in DMSO and *in cellulo* compared to in dioxane and on aggregate formation in aqueous environments. Noteworthy, the radiative decay is rather stronger than the non-radiative process from the CS state *in cellulo*, adding to the potential of such dye-dyads as intracellular fluorescent probes. Conceptually, the study presented is – to the best of our knowledge – the first study of light-induced dynamics of a BODIPY-based dyad in live cells using time-resolved transient absorption spectroscopy. As such, it outlines a promising strategy to evaluate the performance of functional light-driven molecular components in a complex biological environment.

Experimental Section

Transient absorption spectra were obtained with a home-built setup.[27] 530 nm pump beam of ca. 110 fs pulse duration with 500 Hz repetition rate and a white-light probe beam with 1 kHz repetition rate were temporally and spatially focused on the sample position. The polarization between the pump and probe beam was set at a magic angle (ca. 54.7°). 1 cm quartz cuvettes were employed for the solution samples.

For the live cells experiments, 530 nm beam was also used as pump pulse, while the probe wavelengths were set at 4 different narrow regions, for example, 580, 650, 700, 800 nm. The cells were incubated in glass bottom μ-dishes. During the measurements, the MCF-7 cells were treated with 100 μM **BODIPY-Per** for 17 h, and measured in 1 mL Hanks' balanced salt solution (HBSS). Following the measurements, the cells were treated with trypan blue solution and imaged by a combination of Raspberry Pi camera and carl Zeiss Axiovert 25 microscope with the objective EC Plan-Neofluar 10× /0.30 M27 (Figure S5).

The live MCF-7 cells were co-stained with **BODIPY-Per** and Hoechst 33342 nuclear dye. The images were collected by a Leica DMi8 confocal microscope with a 63x oil immersion lens and a heated state at 37 °C. The excited wavelength was set at 488 nm and emission was collected between 600 and 780 nm.

The photo- and dark-cytotoxicity experiments were carried on with a BMG LABTECH CLARIOstar plate absorbance reader. The MCF-7 cells were seeded in a 96-well plate (Nunc) and treated with alamarBlue assay for measuring the cell viabilities. For the dark-cytotoxicity testing at 100 μM **BODIPY-per**, MCF-7 cells were seeded in a Corning Costar 6 well plate and counted by using EVE™ automated cell counter (NanoEnTek).

Conflict of Interest

There are no conflicts to declare.

Data Availability Statement

The data that support the findings of this study are available from the corresponding author upon reasonable request.

[1] a) T. Kowada, H. Maeda, K. Kikuchi, *Chem. Soc. Rev.* **2015**, *44*, 4953–4972; b) S. Adhikari, J. Moscatelli, E. M. Smith, C. Banerjee, E. M. Puchner, *Nat. Commun.* **2019**, *10*, 3400.

[2] a) C. Wang, Y. Qian, *Biomater. Sci.* **2020**, *8*, 830–836; b) V. N. Nguyen, Y. Yim, S. Kim, B. Ryu, K. M. K. Swamy, G. Kim, N. Kwon, C. Y. Kim, S. Park, J. Yoon, *Angew. Chem. Int. Ed. Engl.* **2020**, *59*, 8957–8962.

[3] a) A. Loudet, K. Burgess, *Chem. Rev.* **2007**, *107*, 4891–4932; b) N. Boens, V. Leen, W. Dehaen, *Chem. Soc. Rev.* **2012**, *41*, 1130–1172; c) G. Toupalas, J. Karlsson, F. A. Black, A. Masip-Sanchez, X. Lopez, Y. Ben M'Barek, S. Blanchard, A. Proust, S. Alves, P. Chabera, I. P. Clark, T. Pullerits, J. M. Poblet, E. A. Gibson, G. Izzet, *Angew. Chem. Int. Ed. Engl.* **2021**, *60*, 6518–6525.

[4] a) C. B. Kc, G. N. Lim, V. N. Nesterov, P. A. Karr, F. D'Souza, *Chem. Eur. J.* **2014**, *20*, 17100–17112; b) M. A. Filatov, S. Karuthedath, P. M. Polestshuk, S. Callaghan, K. J. Flanagan, M. Telitchko, T. Wiesner, F. Laquai, M. O. Senge, *Phys. Chem. Chem. Phys.* **2018**, *20*, 8016–8031; c) N. Kiseleva, M. A. Filatov, M. Oldenburg, D. Busko, M. Jakoby, I. A. Howard, B. S. Richards, M. O. Senge, S. M. Borisov, A. Turshatov, *Chem. Commun.* **2018**, *54*, 1607–1610.

[5] a) M. A. Filatov, *Org. Biomol. Chem.* **2019**, *18*, 10–27; b) M. A. Filatov, S. Karuthedath, P. M. Polestshuk, S. Callaghan, K. J. Flanagan, T. Wiesner, F. Laquai, M. O. Senge, *ChemPhotoChem* **2018**, *2*, 606–615; c) Y. Liu, J. Zhao, A. Iagatti, L. Bussotti, P. Foggi, E. Castellucci, M. Di Donato, K.-L. Han, *J. Phys. Chem. C* **2018**, 2502–2511.

[6] a) D. Tian, F. Qi, H. Ma, X. Wang, Y. Pan, R. Chen, Z. Shen, Z. Liu, L. Huang, W. Huang, *Nat. Commun.* **2018**, *9*, 2688; b) P. Maity, T. Gayathri, J. Dana, S. P. Singh, H. N. Ghosh, *J. Photochem. Photobiol. A* **2019**, *368*, 147–152.

[7] a) R. R. Hu, E. Lager, A. Aguilar-Aguilar, J. Z. Liu, J. W. Y. Lam, H. H. Y. Sung, I. D. Williams, Y. C. Zhong, K. S. Wong, E. Pena-Cabrera, B. Z. Tang, *J. Phys. Chem. C* **2009**, *113*, 15845–15853; b) R. Hu, C. F. Gomez-Duran, J. W. Lam, J. L. Belmonte-Vazquez, C. Deng, S. Chen, R. Ye, E. Pena-Cabrera, Y. Zhong, K. S. Wong, B. Z. Tang, *Chem. Commun.* **2012**, *48*, 10099–10101.

[8] a) P. Ashokkumar, A. H. Ashoka, M. Collot, A. Das, A. S. Klymchenko, *Chem. Commun.* **2019**, *55*, 6902–6905; b) H. Zhu, J. Fan, M. Li, J. Cao, J. Wang, X. Peng, *Chem. Eur. J.* **2014**, *20*, 4691–4696.

[9] a) D. Dziuba, P. Jurkiewicz, M. Cebecauer, M. Hof, M. Hocek, *Angew. Chem. Int. Ed. Engl.* **2016**, *55*, 174–178; b) Z. Yang, Y. He, J. H. Lee, W. S. Chae, W. X. Ren, J. H. Lee, C. Kang, J. S. Kim, *Chem. Commun.* **2014**, *50*, 11672–11675.

[10] J. Banuelos, *Chem. Rec.* **2016**, *16*, 335–348.

[11] a) D. Kand, P. Liu, M. X. Navarro, L. J. Fischer, L. Rousso-Noori, D. Friedmann-Morvinski, A. H. Winter, E. W. Miller, R. Weinstain, *J. Am. Chem. Soc.* **2020**, *142*, 4970–4974; b) X. Miao, H. Tao, W. Hu, Y. Pan, Q. Fan, W. Huang, *Sci. China Chem.* **2020**, *63*, 1075–1081; c) S. L. Niu, G. Ulrich, R. Ziessel, A. Kiss, P. Y. Renard, A. Romieu, *Org. Lett.* **2009**, *11*, 2049–2052; d) Z. Zhao, Z. Chang, B. He, B. Chen, C. Deng, P. Lu, H. Qiu, B. Z. Tang, *Chem. Eur. J.* **2013**, *19*, 11512–11517.

[12] a) S. Choi, J. Bouffard, Y. Kim, *Chem. Sci.* **2014**, *5*, 751–755; b) W. Che, G. Li, J. Zhang, Y. Geng, Z. Xie, D. Zhu, Z. Su, *J. Photochem. Photobiol. A* **2018**, *358*, 274–283.

[13] a) H. Sunahara, Y. Urano, H. Kojima, T. Nagano, *J. Am. Chem. Soc.* **2007**, *129*, 5597–5604; b) M. A. Filatov, S. Karuthedath, P. M. Polestshuk, H. Savoie, K. J. Flanagan, C. Sy, E. Sitte, M. Telitchko, F. Laquai, R. W. Boyle, M. O. Senge, *J. Am. Chem. Soc.* **2017**, *139*, 6282–6285; c) F. M. Santos, J. N. Rosa, N. R. Candeias, C. P. Carvalho, A. I. Matos, A. E. Ventura, H. F. Florindo, L. C. Silva, U. Pischel, P. M. Gois, *Chem. Eur. J.* **2016**, *22*, 1631–1637.

[14] a) T. Mosmann, *J. Immunol. Methods* **1983**, *65*, 55–63; b) K. H. Liao, Y. S. Lin, C. W. Macosko, C. L. Haynes, *ACS Appl. Mater. Interfaces* **2011**, *3*, 2607–2615.

[15] a) J. Galvao, B. Davis, M. Tilley, E. Normando, M. R. Duchen, M. F. Cordeiro, *FASEB J.* **2013**, *28*, 1317–1330; b) L. Jamalzadeh, H. Ghafoori, R. Sariri, H. Rabuti, J. Nasirzade, H. Hasani, M. R. Aghamaali, *Avicenna J. Med. Biochem.* **2016**, *4*, 10–33453.

[16] a) D. Plesca, S. Mazumder, A. Almasan in *Programmed Cell Death, The Biology and Therapeutic Implications of Cell Death, Part B*, **2008**, pp. 107–122; b) M. J. Abedin, D. Wang, M. A. McDonnell, U. Lehmann, A. Kelekar, *Cell Death Differ* **2007**, *14*, 500–510.

[17] J. T. Buck, A. M. Boudreau, A. DeCarmine, R. W. Wilson, J. Hampsey, T. Mani, *Chem* **2019**, *5*, 138–155.

[18] J. Karolin, L. B. A. Johansson, L. Strandberg, T. Ny, *J. Am. Chem. Soc.* **1994**, *116*, 7801–7806.

[19] A. M. Lifschitz, R. M. Young, J. Mendez-Arroyo, V. V. Roznyatovskiy, C. M. McGuirk, M. R. Wasielewski, C. A. Mirkin, *Chem. Commun.* **2014**, *50*, 6850–6852.

[20] Z. Wang, M. Ivanov, Y. Gao, L. Bussotti, P. Foggi, H. Zhang, N. Russo, B. Dick, J. Zhao, M. Di Donato, G. Mazzone, L. Luo, M. Fedin, *Chem. Eur. J.* **2020**, *26*, 1091–1102.

[21] a) K. Li, X. Duan, Z. Jiang, D. Ding, Y. Chen, G. Q. Zhang, Z. Liu, *Nat. Commun.* **2021**, *12*, 2376; b) T. Kim, W. Kim, O. Vakuliuk, D. T. Gryko, D. Kim, *J. American Chem. Soc.* **2019**, *142*, 1564–1573.

[22] a) J. L. Bredas, J. E. Norton, J. Cornil, V. Coropceanu, *Acc. Chem. Res.* **2009**, *42*, 1691–1699; b) R. J. Willemse, D. Theodori, J. W. Verhoeven, A. M. Brouwer, *Photochem. Photobiol. Sci.* **2003**, *2*, 1134–1139.

[23] T. Asahi, M. Ohkohchi, R. Matsusaka, N. Mataga, R. P. Zhang, A. Osuka, K. Maruyama, *J. Am. Chem. Soc.* **1993**, *115*, 5665–5674.

[24] M. Sittig, B. Schmidt, H. Gorls, T. Bocklitz, M. Wachtler, S. Zechel, M. D. Hager, B. Dietzek, *Phys. Chem. Chem. Phys.* **2020**, *22*, 4072–4079.

[25] X. Song, N. Li, C. Wang, Y. Xiao, *J. Mater. Chem. B* **2017**, *5*, 360–368.

[26] T. Yang, A. Chettri, B. Radwan, E. Matuszyk, M. Baranska, B. Dietzek, *Chem. Commun.* **2021**, *57*, 6392–6395.

[27] R. Siebert, D. Akimov, M. Schmitt, A. Winter, U. S. Schubert, B. Dietzek, J. Popp, *ChemPhysChem* **2009**, *10*, 910–919.